

Available online at [www.sciencedirect.com](http://www.sciencedirect.com)**ScienceDirect**

Procedia Engineering 184 (2017) 298 – 305

---

**Procedia  
Engineering**

---

[www.elsevier.com/locate/procedia](http://www.elsevier.com/locate/procedia)

Advances in Material &amp; Processing Technologies Conference

## Effect of Different Cooling Rates Condition on Thermal Profile and Microstructure of Aluminium 6061

B. Benjunior<sup>a,b</sup>, A.H. Ahmad<sup>a,b\*</sup>, Maarof Mohd. Rashidi<sup>a,b</sup>, M.S. Reza<sup>a,b</sup><sup>a</sup>*Faculty of Mechanical Engineering, Universiti Malaysia Pahang, Malaysia*<sup>b</sup>*Manufacturing Process Group, University Malaysia Pahang, Malaysia*

---

### Abstract

Thermal analysis and microstructure characterization provide information regarding material thermal profiles and microstructure formation. Wrought aluminium alloys offer significant advantages in terms of higher ultimate tensile strength (UTS) and yield strength but relatively poor fluidity properties. The objective of this experiment presented in this paper was to understand the relationship between solidification rate, metallurgical behaviour, and fraction phase growth of wrought aluminium 6061. This information was crucial and important to the foundry industry to understand the material behaviour that will help to cast wrought aluminium 6061. Thermal analysis and microstructure of wrought aluminium 6061 on different cooling conditions are present in this paper. In this work, Aluminium 6061 heated and melted in a graphite crucible at a temperature of 800 °C. Two thermocouples located at the centre and 20 mm from the graphite crucible wall. Slow cooling rate condition experiment rig was developed by placing graphite crucible into a chamber with kaowool insulation. Normal cooling rate condition was developed by allowing the molten solidify at room temperature. Fast cooling rate condition was prepared by applying a forced airflow over the graphite crucible. The slow, normal, and high cooling rates were calculated at 0.03 °C/s, 0.2 °C/s and 0.3 °C/s respectively. Cooling curve analysis was performed to predict various areas of solidification phase and fraction solid. In Addition, the microstructure formation was observed, recorded, and compared between different cooling conditions. The results show slow cooling rate condition formation of eutectic and solidus temperatures occurred far from liquidus temperature. The eutectic and solidus temperature was increased with the increment of the cooling rate. Furthermore, the DCP temperature of slow cooling rate condition at 638.3 °C was the lowest while gives wider temperature range corresponding to the fraction solid percentage increment. Meanwhile, an increase in cooling rate refined the microstructure, improved the grain circularity and at the same time reduced the aspect ratio.

© 2017 The Authors. Published by Elsevier Ltd. This is an open access article under the CC BY-NC-ND license (<http://creativecommons.org/licenses/by-nc-nd/4.0/>).

Peer-review under responsibility of the organizing committee of the Urban Transitions Conference

**Keywords:** Cooling Rates; Thermal Profile; Microstructure; Aluminium Alloy 6061; Fraction Solid;

---

**Nomenclature**

C	circularity
A	area
P	perimeter
AR	aspect ratio

**1. Introduction**

Nowadays, aluminium alloys is an ideal material to be used for automotive, aerospace and transportation components with casting alloy such as A356 due to their fluidity behaviour. However, while the cast series of aluminium alloys has the excellent fluidity properties advantage, it has relatively poor mechanical properties compared to wrought aluminium alloys. Wrought aluminium alloys provide significant advantages in terms of higher ultimate tensile strength (UTS) and yield strength. Wrought aluminium alloy 6061 is among the wrought alloy series that known to have various benefits of medium strength, formability, weldability low cost and also corrosion resistance [1].

Qualities of the molten alloy usually control and characterise by two inspection methods which are microstructure and elemental chemical measurement. Thermal analysis (TA) is an alternative suitable and essential characterization method which allows determination of the quality of a melt batch through footage of phase change temperatures and fraction solid-temperature summaries [2]. The term TA is referred as analysing the change in a property of a material under different temperature modifications [3]. Differential thermal analysis (DTA) and differential scanning calorimetry (DSC) are among a list of thermal analysis methods that commonly being used. Both of these methods use a sample to be tested and a reference sample. DTA theory is by computing variations of temperature in the sample, DSC however, dealings with calculating the energy difference between the samples directly [4].

Alternative thermal analysis method uses two thermocouples to measure the heat change in a single sample. Previous study state that the temperature variance between the solidification cooling curves at two different points within the melt can be used to determine the dendritic coherency points (DCP) [4, 5]. The DCP shows the point during solidification where the dendrites are starting to interrupt on one another through the solidifying system and also where the metal strength properties are starting to progress [5, 6]. Before DCP, the solidifying metal has insignificant shear strength compared to after DCP occurs where the dendritic network has formed and developed. Therefore, this point is accompanied by a significant increase system viscosity and strength [6].

Cooling curve analysis is analysed based on the thermal application to the material let it be heating or cooling, and it is directly related to phase transformation of the material during the cooling process [7]. Therefore, solid fractions of the material can be determined based on its cooling curve. The cooling curve analysis method is to analyse temperature versus time during the solidification of the heated aluminium. The data is analysed using computer-aided cooling curve analysis (CA-CCA) in order to determine the thermo-physical properties of the aluminium alloy, the latent heat and solid fraction [8].

Microstructure inspection is one of the methods to control and characterise the melt. Previous studies have revealed that cooling rate gives significant effect to microstructure formation where higher cooling rate gives more refined microstructure, increase the strength of impact and hardness [9, 10]. In addition, higher cooling rates produced a finer primary  $\alpha$ -phase particle [10, 11]. The cooling rate is also the main factor to affect the temperature gradient and solidification rate and vital variables which affect microstructure and mechanical properties of castings [12]. The objective of this experiment presented in this paper was to understand the relationship between solidification rate, metallurgical behaviour, and fraction phase growth of wrought aluminium 6061.

## 2. Experimental Method

Table 1: Chemical composition of the aluminium alloy 6061.

Composition	Al	Si	Fe	Cu	Mn	Mg	Zn	Cr	Ni	Ti
Wt (%)	97.400	1.00	0.290	0.030	0.530	0.570	0.009	0.011	0.019	0.020

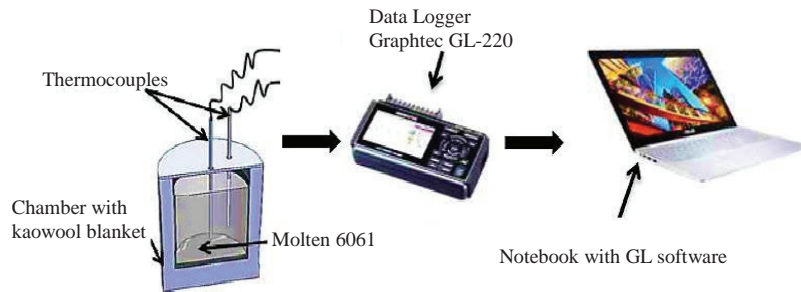


Figure 1: Schematic Diagram of Experiment Rig for Slow Cooling Condition

Table 1 present Chemical compositions of aluminium 6061 determined by using Optical Emission Spectrometer. The aluminium 6061 was placed inside a graphite crucible and was then melted by using a resistance heated Carbolite 1600 box furnace at a temperature of 800 °C. The experimental rig for slow cooling rate condition was developed by using a wooden chamber with kaowool blanket as heat lost insulation to achieve a slow cooling rate condition. The molten aluminium 6061 then was placed into this rig and allowed to solidify. The intermediate cooling rate condition was conducted by allowing the molten to cool naturally at room temperature. The schematic diagram for the slow cooling rate condition experimental rig is presented in Figure 1. The fast cooling rate condition was achieved by fan blower forced air through graphite crucible with molten alloy inside. The temperature of the molten was measured by using two pieces of k-type thermocouple immersed about half into the molten metal height in the graphite crucible. The thermocouples were positioned at the centre and 20 mm from the crucible wall respectively. The thermocouples were connected to a Data Logger GL-220 which linked to a notebook. The data logger was set at 10 Hz/ch.

The cooling curve graph of temperature against time from different cooling condition was plotted. From the cooling curve obtained the first derivative graph was calculated. The zero-curve of the graph is determined after the first derivative of the graph was obtained. The base line of the graph was obtained from the differential temperature of liquidus and solidus from the first derivative graph using third order polynomial. The solid fraction was calculated based on the first derivative and baseline graph. The microscopic samples were then taken at the centre of solidified alloy at 20 mm from the top of the graphite crucible. The sample was then mount by using SimpliMet 1000 Automatic Mounting press mounting machine and grind by using Metkon Forcipol 2V grinding machine with the rotation of 240-300rpm and grit specification P240, P600, P800 and P1200 of abrasive paper respectively. The sample was polished and etched with Keller solution and microstructure image of the sample were taken. The microstructure image was analyzed with ImageJ software in order to obtain grain size area, circularity and aspect ratio. The circularity and aspect ratio were calculated with Equation 1 and Equation 2 where P and A are representing a perimeter and an area of the particle respectively:

$$C = 4\pi A/P^2 \quad (1)$$

$$AR = \text{major axis}/\text{minor axis} \quad (2)$$

### 3. Results and Discussion

#### 3.1 Thermal analysis

The cooling curve regression method was used to determine aluminium 6061 thermal profile. Figure 2 presents result from the slow cooling rate condition (0.03 °C/s). The expanded region shows a phase in which the sample was in the transition phase from liquid to solid. During primary phase precipitation, a large amount of latent heat was released, causes a rapid drop in temperature. Meanwhile, in secondary phase precipitation, small quantities of latent heat was released thus solid state region occur. Derivation curve allows identification of the phase changes that took place in the alloys during the solidification period. Baseline curve is a third order polynomial line plotted on the graph when cooling process is assumed not to undergo a phase transformation. Figure 2 (b) shows a derivative curve for slow cooling rate, which liquidus temperature starts to develop at 626 °C. The eutectic temperature occurred at 621 °C and solidus temperature began at 554 °C.

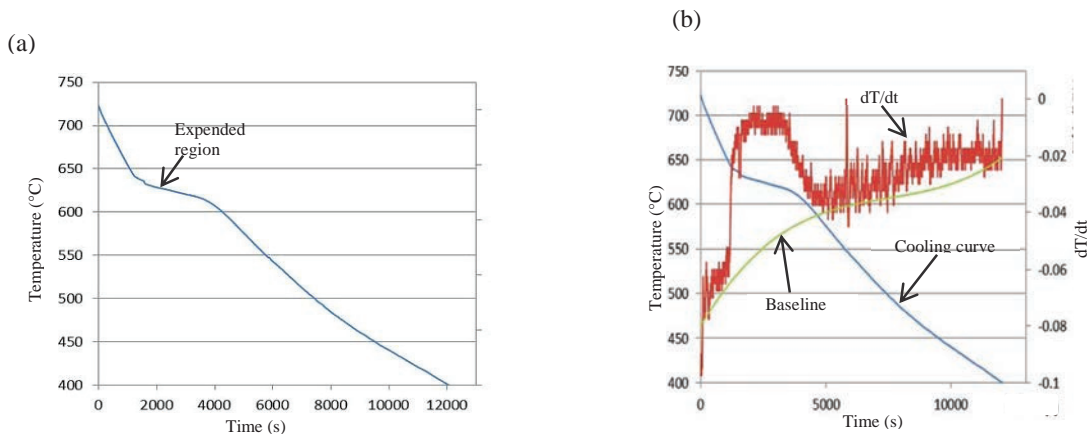


Figure 2: Slow cooling rate (0.03 °C/s) with (a) cooling curve and (b) cooling rate with 1<sup>st</sup> derivation.

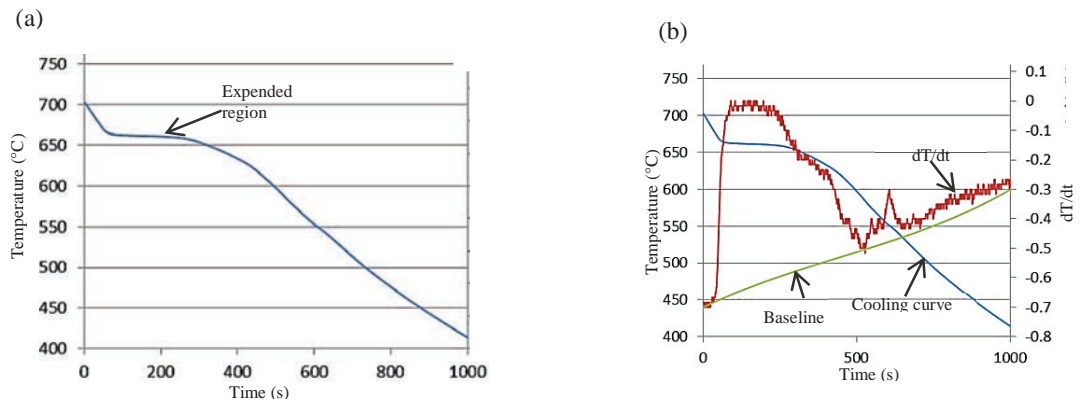


Figure 3: Intermediate cooling rate (0.2 °C/s) with (a) cooling curve and (b) cooling rate with 1<sup>st</sup> derivation.

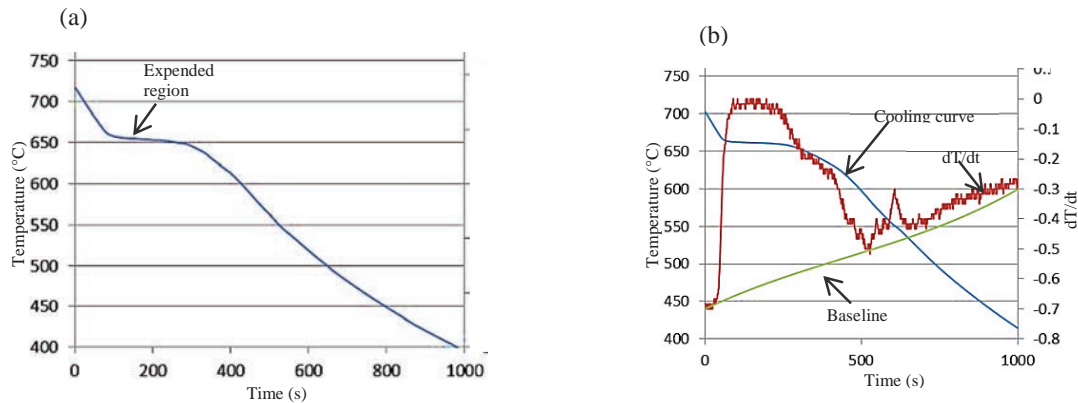


Figure 4: Fast cooling rate (0.3 °C/s) with (a) cooling curve and (b) cooling rate with 1<sup>st</sup> derivation.

Figure 3 expresses cooling curve from the intermediate cooling rate condition (0.2 °C/s). While Figure 3 (b) shows derivative curve for intermediate cooling rate which the formation of liquidus temperature was started at 663.6 °C. The eutectic temperature occurred at 661.8 °C and the solidus temperature was at 551.2 °C.

The fast cooling rate condition cooling curve is presented in Figure 4 at 0.3 °C/s cooling rate condition. Where else, Figure 4 (b) shows the derivative curve for 0.3 °C/s cooling rate condition where the formation of liquidus temperature was started at 659.6 °C. The eutectic temperature occurred at 653 °C and the solidus temperature began at 541.3 °C.

### 3. 5 Dendritic coherency point (DCP)

The two thermocouples technique was developed specifically to measure DCP of the sample. DCP occurred when there was a rapid decrease in the temperature difference between the wall and the centre of the crucible. The result shows that the DCP temperature was increased from a temperature of 638.3 °C to 657.6 °C for a cooling rate increase from 0.03 °C/s to 0.2 °C/s respectively. However, it was found that the DCP temperature change was not significant for a further increase in cooling rate from 0.2 °C/s to 0.3 °C/s. The results indicate that when the cooling rate increased, the formation of dendrites was much faster, which produced DCP at a higher temperature. Heat extracted from molten 6061 was faster at higher cooling rates than slow cooling rate due to insulation effect.

### 3. 4 Effect of cooling rate on solidification and fraction solid

Experimental results show that higher cooling rate caused faster solidification of aluminium 6061. Table 2 compares results between different cooling rate conditions and their fraction solid percentage with the corresponding temperature. There was a narrow range of temperature dropped compared to the increment in fraction solid percentage at a cooling rate of 0.2 °C/s and 0.3 °C/s. However, for the cooling rate of 0.03 °C/s, the fraction solid percentage increment takes a longer time and at a lower temperature compared to cooling rates at 0.2 °C/s and 0.3 °C/s. This indicates that in the slow cooling rate the formation of eutectic and solidus temperatures occurred far from liquidus temperature. The eutectic and solidus temperature was increased with the increment of the cooling rate. This result was consistent with other reported results found by the previous researcher on wrought aluminium alloy fraction solid percentage was higher at a higher temperature by increasing the cooling rates [5, 13].

### 3. 6 Effect of cooling rate on dendrite coherency point (DCP)

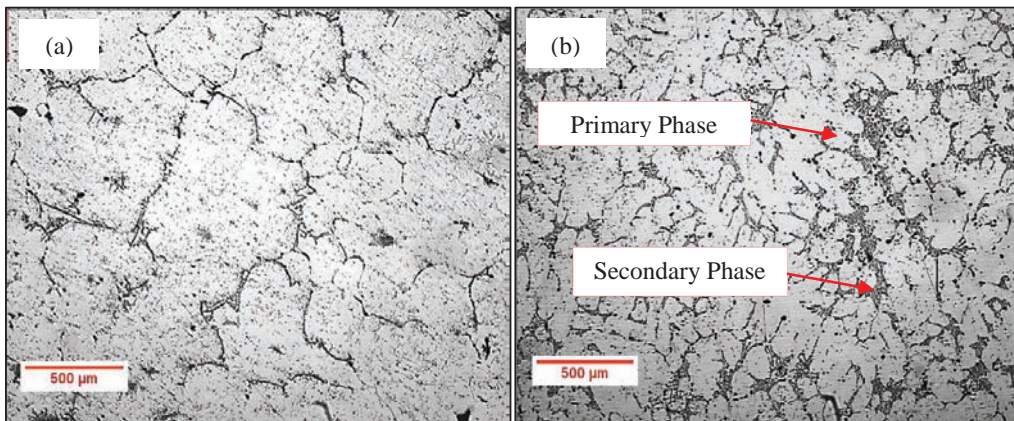
In SSM processing, it is vital to have an understanding in DCP. The shear strength of the semi-solid material increases significantly after this point. Understanding this point, hence gives a better understanding of material behaviour and lead to a more specific in the determination of a suitable temperature for processing. Previously, an optimum fraction solid for thixoforging is renowned to be within the range of 0.3 to 0.5 [14, 15]. By exploitation of a lower cooling rate, DCP can be adjusted to a lower temperature and higher fraction solid with the advantage of extending the temperature and fraction solid range over which the semi-solid material can be processed [6]. The result of this experimental work shows that the DCP temperature of slow cooling rate condition at 638.3 °C was the lowest while gives wider temperature range corresponding to the fraction solid percentage increment. By altering the cooling rates to slow condition, the DCP temperature was extended to a lower temperature while produce higher fraction solid percentage over a wider temperature range.

Table 2: Fraction Solid of 0.03 °C/s, 0.2 °C/s and 0.3 °C/s Cooling Rate with percentage of 20 %, 40 % and 60 %.

Cooling rate (°C/s)	Fraction solid (%)	Temperature (°C)
0.03	20	615
	40	609
	60	606
0.2	20	662
	40	661
	60	659
0.3	20	655
	40	654
	60	652

### 3. 7 Effect of cooling rate on microstructure

Figure 5 (a), Figure 5 (b), and Figure 5 (c) shows the microstructure results obtained from a cooling rate of 0.03 °C/s, 0.2 °C/s, and 0.3 °C/s respectively. The result shows obvious differentiation that higher cooling rate produced finer grain size, which consistent with the literature review on the previous study on the effect of cooling rates on aluminium alloy microstructure [5, 10, 16]. The two important phases in the microstructure are the primary phase that solidifies first and the secondary phase that solidifies second was labelled in Figure 5 (b). In general, a microstructure with more secondary phase will have higher fluidity.



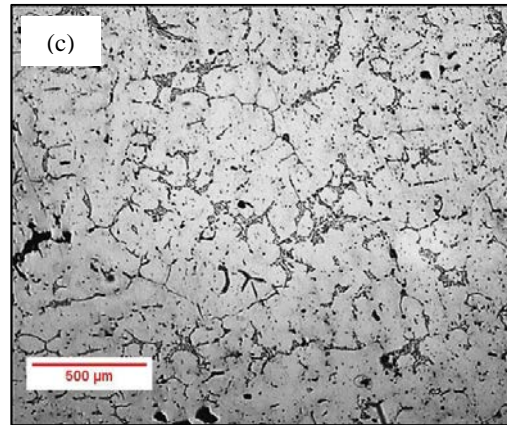


Figure 5: Microstructure of (a) Slow cooling rate (0.03 °C/s), (b) Intermediate cooling rate (0.2 °C/s), and (c) Fast cooling rate (0.3 °C/s).

Table 3 shows the significant difference in grain size area and grain circularity between slow and fast cooling rates condition. Fast cooling rate condition produced smallest grain size with higher circularity that is  $5057.11 \mu\text{m}^2$  and 0.7 circularity measurement respectively. This result was similar and consistent with other researcher finding which stated that the incremental in cooling rate not just created finer microstructure but in the same time reduce the shape factor in term of the aspect ratio. The shape factor in term of circularity was also improved although it is not significant. [ 5, 16-17]

Table 3: Grain Size Area and Grain Circularity between Different Cooling Rates.

Cooling Rate	Grain Size Area ( $\mu\text{m}^2$ )	Circularity	Aspect Ratio
Slow	42121.39	0.647292	1.776583
Fast	5057.11	0.708792	1.468292

#### 4. Conclusion

The investigation on the effect of different cooling rates on thermal profile and microstructure of aluminium 6061 was studied in this experiment. In conclusion, different cooling rates condition will alter the material phase changes temperature. Slow cooling rate condition (0.03 °C/s) primary  $\alpha$ -Al starts to occurred at 626 °C and the primary eutectic solidification occurred at a 621°C. Fast cooling rate condition (0.3 °C/s) primary  $\alpha$ -Al starts occurred at 659.6 °C and the primary eutectic solidification occurred at a 653°C. DCP temperature for slow cooling rate are lower which formed at temperature 638.3°C compared to fast cooling rate DCP temperature at 648.8 °C. This was due to the solidification time and dendritic arms growths rate take longer time. Different cooling rates also affect the microstructure of aluminium alloy 6061 significantly. The microstructure results obtained shown that the fast cooling rate condition produced smaller grain size compared to the slow cooling rate condition grain size.

#### References

- [1] S.H. Lee, Y. Saito, T. Sakai, H. Utsunomiya, *Materials Science and Engineering: A* 325 (2002) 228-235.
- [2] D. Emadi, L. Whiting, S. Nafisi, R. Ghomashchi, *Journal of thermal analysis and calorimetry* 81 (2005) 235-242.
- [3] M.E. Brown, *Introduction to Thermal Analysis, Volume 2 : Techniques and Applications* (2nd Edition), Kluwer Academic Publishers, Secaucus, NJ, USA, 2001.
- [4] A.H. Ahmad, S. Naher, D. Brabazon, *Thermal profiles and fraction solid of aluminium 7075 at different cooling rate conditions*, *Key Engineering Materials*, vol 554, Trans Tech Publ, 2013, pp. 582-595.
- [5] L. Backerud, G. Chai, J. Tamminen, *American Foundrymen's Society, Inc.*, 1990 (1990) 266.
- [6] A. Dahle, D. StJohn, *Acta materialia* 47 (1998) 31-41.
- [7] Ihsan-ul-haq, J.-S. Shin, Z.-H. Lee, *METALS AND MATERIALS International* 10 (2004) 89-96.

- [8] M. Dehnavi, F. Kuhestani, M. Haddad-Sabzevar, (2015) 196-205.
- [9] K.T. Akhil, S. Arul, R. Sellamuthu, Procedia Materials Science 5 (2014) 362-368.
- [10] A. Ahmad, S. Naher, D. Brabazon, International Journal of Automotive and Mechanical Engineering 9 (2014) 1685.
- [11] N.K. Kund, Transactions of Nonferrous Metals Society of China 25 (2015) 61-71.
- [12] R. Chen, Y.-f. Shi, Q.-y. Xu, B.-c. Liu, Transactions of Nonferrous Metals Society of China 24 (2014) 1645-1652.
- [13] Hosseini, V.A., Shabestari, S.G. and Gholizadeh, R., 2013. Study on the effect of cooling rate on the solidification parameters, microstructure, and mechanical properties of LM13 alloy using cooling curve thermal analysis technique. Materials & Design, 50(0), pp. 7-14.
- [14] A.M. Camacho, H. Atkinson, P. Kapranos, B. Argent, Acta Materialia 51 (2003) 2319-2330.
- [15] T. Haga, P. Kapranos, Journal of Materials Processing Technology 130 (2002) 594-598.
- [16] Shabestari, S. G., and M. Malekan. "Thermal analysis study of the effect of the cooling rate on the microstructure and solidification parameters of 319 aluminum alloy." Canadian Metallurgical Quarterly 44.3 (2005): 305-312.
- [17] Bünck, Matthias, Nils Warnken, and Andreas Bührig-Polaczek. "Microstructure evolution of rheo-cast A356 aluminium alloy in consideration of different cooling conditions by means of the cooling channel process." Journal of Materials Processing Technology 210.4 (2010): 624-630.